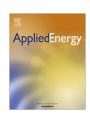
ELSEVIER

Contents lists available at ScienceDirect

Applied Energy

journal homepage: www.elsevier.com/locate/apenergy



Novel methods for estimating lithium-ion battery state of energy and maximum available energy



Linfeng Zheng a,b,*, Jianguo Zhu a, Guoxiu Wang b, Tingting He a, Yiying Wei a,b

^a Faculty of Engineering and Information Technology, University of Technology Sydney, Sydney, N.S.W. 2007, Australia

HIGHLIGHTS

- Study on temperature, current, aging dependencies of maximum available energy.
- Study on the various factors dependencies of relationships between SOE and SOC.
- A quantitative relationship between SOE and SOC is proposed for SOE estimation.
- Estimate maximum available energy by means of moving-window energy-integral.
- The robustness and feasibility of the proposed approaches are systematic evaluated.

ARTICLE INFO

Article history: Received 11 April 2016 Received in revised form 1 June 2016 Accepted 11 June 2016

Keywords:
Battery management system (BMS)
State of energy (SOE)
State of charge (SOC)
Maximum available energy

ABSTRACT

The battery state of energy (SOE) allows a direct determination of the ratio between the remaining and maximum available energy of a battery, which is critical for energy optimization and management in energy storage systems. In this paper, the ambient temperature, battery discharge/charge current rate and cell aging level dependencies of battery maximum available energy and SOE are comprehensively analyzed. An explicit quantitative relationship between SOE and state of charge (SOC) for LiMn₂O₄ battery cells is proposed for SOE estimation, and a moving-window energy-integral technique is incorporated to estimate battery maximum available energy. Experimental results show that the proposed approaches can estimate battery maximum available energy and SOE with high precision. The robustness of the proposed approaches against various operation conditions and cell aging levels is systematically evaluated.

© 2016 Elsevier Ltd. All rights reserved.

1. Introduction

Lithium-ion batteries have many desirable merits such as high energy density, light weight and long cycle life, and are widely developed as energy storage devices in smart grids and electric vehicles [1,2], etc. To meet the application power and energy demands, a battery system usually contains hundreds, even thousands of cells connected in series and parallel. To ensure safe and reliable operation, an effective battery management system (BMS) is required to monitor and control these cells. Much of the BMS functionalities, such as the state of charge (SOC) estimation, state of health estimation, cell monitoring and balancing techniques [3–8], have been sophisticatedly developed for applications. Nevertheless, due to the nonlinear battery characteristics and unpredictable operating conditions, accurate and reliable battery

E-mail address: Linfeng.Zheng@student.uts.edu.au (L. Zheng).

state of energy (SOE) and maximum available energy estimations still pose significant challenges.

Traditionally, the SOC is regarded as an indicator of battery available energy. A wide variety of approaches for SOC estimation has been reported in recent literature [2,9-19], and remarkable results have been achieved on novel SOC estimation methods and improving the estimated accuracy. For example, the proportional-integral (PI) observer [11], Luenberger observer [12,13], Sliding-mode observer [14,15] and Kalman-filter-based algorithms [2,16-19] were employed in model-based SOC estimation methods to obtain estimated results of high accuracy. Defined as the ratio of the remaining charge stored in a battery to its full capacity, however, SOC actually indicates the state of available capacity rather than the state of available energy. Mamadou et al. [20,21] introduced a new criterion, state of energy (SOE), for battery energetic performances evaluation. SOE allows a direct determination of the ratio of battery remaining energy to its maximum available energy, which is critical for energy optimization and management in energy storage systems.

^b Centre for Clean Energy Technology, University of Technology Sydney, Sydney, N.S.W. 2007, Australia

^{*} Corresponding author at: Faculty of Engineering and Information Technology, University of Technology Sydney, Sydney, N.S.W. 2007, Australia.

Compared with the SOC estimation approaches, there are few studies report the systematic research for SOE estimation. Refs. [22,23] presented SOE estimation methods based on Neural Network, which treats the target battery as a "black-box" system and needs a great number of sample data to train the network parameters. The main disadvantage of this method is that the estimation errors are strongly dependent on the training data. In [24,25], an adaptive unscented Kalman filter algorithm and the relationship between the SOE and open circuit voltage (OCV) were employed in the model-based SOE estimation approaches. In [26], the particle filter and a battery model are utilized to develop a method for joint estimation of the SOE and the SOC, and the robustness of the method has been verified under dynamic temperature conditions. He et al. [27] employed a Gaussian model oriented battery model and proposed a data-driven estimator with a central difference Kalman filter algorithm for SOE estimation, and the approach was evaluated by two kinds of batteries including LiFePO₄ and LiMn₂O₄ cells. Although these SOE estimation approaches are able to achieve acceptable accuracy, the complex algorithms produce a heavy computational burden on the microprocessor with limited computation capability within BMSs.

Besides, a common drawback of these SOE estimation methods is that they fail to achieve desirable predictions against various operating conditions during battery aging processes. The trajectory of the neural network parameters or battery model parameters cannot be fully described within a limited number of experiments [27]. Various battery operating conditions and cell aging levels with pre-set parameters may lead to inaccurate SOE estimated results. It is also noted that the above-mentioned battery available energy studies focus just on the SOE estimation. Unfortunately, there are very few studies involving the estimation of battery maximum available energy (i.e. battery actual energy). Since the battery maximum available energy is strongly related to the battery operating conditions [22], it is necessary to systematically study the effects of ambient temperature, current rate, and aging level in order to estimate the SOE and maximum available energy more accurately, and further improve the robustness of estimation approaches against uncertain operating conditions.

To implement this work, a battery test bench was developed, and the characteristics of $LiMn_2O_4$ battery cells with a nominal capacity of 90 A h were tested under different aging levels, current rates, and ambient temperatures. The tests cover a broad aging level range from 92 A h to 69.5 A h, a wide temperature range from 10 °C to 40 °C and a commonly used current rate range from 1/3 C to 1 C. Based on the test data, the relationships between SOE and SOC under various operating conditions are systematically analyzed and quantified for SOE estimation. A moving-window energy-integral technique is incorporated to estimate the battery maximum available energy. The robustness and feasibility of the proposed approaches are validated in different operating condition tests during battery aging processes.

The remainder of the paper is arranged as follows: Section 2 introduces the battery test bench and analyzes the dependencies of battery available energy and SOE on the temperature, current and cell aging level. Section 3 presents the proposed algorithms of battery SOE and maximum available energy estimations. The experimental results and evaluation of the proposed approaches are reported in Section 4, followed by the conclusions and future work in Section 5.

2. Battery experiments and results

2.1. Battery test bench

The $LiMn_2O_4$ cells with a nominal capacity of 90 A h were used to investigate the battery energy characteristics at various

experimental conditions of different ambient temperatures, current rates, and cell aging levels. A battery test bench was set up to obtain battery characterization experimental data, as shown in Fig. 1.

The battery test bench is composed of a battery charger/discharger, a host computer, a programmable temperature chamber and Lithium-ion battery cells. The battery charger/discharger functions to charge or discharge battery cells according to preset loading profiles and its voltage and current measurement accuracy is 0.05% full scale. The host computer is used to set the loading profiles and control the battery charger/discharger through the TCP/IP communications. It is also used to record a set of real-time battery variables, such as battery terminal voltage, loading current, and charge/discharge energy. The programmable temperature chamber can simulate various ambient temperatures and is used to control the battery operated under the designed temperatures.

2.2. Temperature, current and aging level dependencies of battery maximum available energy

In order to investigate the battery maximum available energy with different currents at various ambient temperatures, the battery cells were loaded with the discharge current rates of C/3, C/3, C/2 and 1 C at temperatures of 10 °C, 25 °C and 40 °C, respectively. At each temperature, the battery cells were firstly charged with a preset constant current to the upper limit voltage 4.2 V followed by a constant voltage charge at 4.2 V until C/20 cutoff. Then, there was a rest time for 1 h followed by the preset constant current discharge to the lower limit voltage 3 V. After that, the battery was given a rest for 1 h and the procedure was carried out repeatedly. During the battery discharge processes, the maximum available energy results with different currents at various temperatures are shown in Fig. 2.

From Fig. 2, it can be found that the battery maximum available energy presents a change with different currents at various temperatures. At the same ambient temperature, the available energy appears a decreasing trend with the increasing discharge current rate. For example, when the discharge current rate was increased from 1/3 C to 1 C, the available energy dropped from 324.8 W h to 315.1 W h at 10 °C. At various temperatures, when the discharge current rate is kept at 1/3 C, the maximum available energies are 324.8 W h, 355.1 W h, and 356.5 W h at 10 °C, 25 °C and 40 °C, respectively, presenting an increasing trend with the rising temperature.

To investigate the battery maximum available energy with different currents at various battery cell aging levels, accelerated aging tests with the charge/discharge current of 1 C at 60 °C were applied to the battery cell to obtain different cell aging levels including 92 A h, 87 A h, 82.5 A h, 78 A h, 74.5 A h and 69.5 A h, and at each cell aging level, the battery cell was loaded with the discharge currents of C/3, C/2, 2 C/3 and 1 C at the room temperature (25 °C), respectively. The battery maximum available energy values are plotted in Fig. 3.

In Fig. 3, when the discharge current rate is 1/3 C, the battery maximum available energy values are 355.1 W h, 331.9 W h, 315.8 W h, 299.0 W h, 281.9 W h and 261.4 W h at the battery capacity 92 A h, 87 A h, 82.5 A h, 78.5 A h, 74 A h and 69.5 A h, respectively. The maximum available energy shows similar declining trends with different discharge current rates such as 1/2 C, 2/3 C, and 1 C at different aging levels, indicating that the battery maximum available energy appears a significant decrease during battery aging processes.

It can be concluded that the battery maximum available energy varies with the operating conditions and is greatly related to the ambient temperature and cell aging level. Accordingly, it is necessary to develop reliable approaches for accurate battery maximum

Download English Version:

https://daneshyari.com/en/article/6682415

Download Persian Version:

https://daneshyari.com/article/6682415

<u>Daneshyari.com</u>